ScientificScholar®
Knowledge is power
Publisher of Scientific Journals

https://arabjchem.org

Arabian Journal of Chemistry

2025 18 (2) 122024

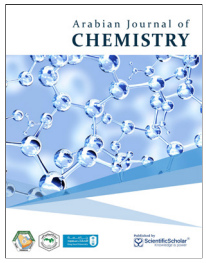

Original Article

Study on explosion characteristics and mechanism of petroleum volatile gas

Yansong Zhang[a], Yunkuan Zhang[a], Xiang Wang[a], Jie Zhang[b], Jing Shi[a], Xiangrui Wei[a,*]

[a]Department of College of Safety and Environmental Engineering, Shandong University of Science and Technology, No. 579 Qianwangang Road, Huangdao District, Qingdao City, Shandong Province, Qingdao, 266590, Shandong, China
[b]Department of College of Safety Science and Engineering, Xi'an University of Science and Technology, No. 58 Yanta Road, Xi'an City, Shaanxi Province, Xi'an, 710054, Shaanxi, China

ARTICLE INFO

Keywords:
Explosion mechanism
Explosive overpressure
Flame propagation speed
Heat loss

ABSTRACT

The explosion characteristics and explosion mechanism of petroleum volatile gas were studied by 20 L spherical explosion experiment and gas explosion flame propagation experiment. The results show that with the increase of the equivalent ratio, the peak explosion pressure and the maximum explosion pressure rise first and then decline. When the equivalent ratio is 1.2, the explosion pressure reaches the maximum. Under different equivalent ratio conditions, the flame propagation trend shows "N" type, and the propagation speed is the fastest when the equivalent ratio is 1.0. During the test of petroleum volatile gas explosion in a closed container, the effect of heat loss on the test results should not be ignored.

1. Introduction

Oil and coal mines are indispensable strategic resources, energy materials, and chemical raw materials in the world [1-3]. The most hazardous accidents in the chemical industry mainly include explosions, toxic substance leaks, etc [4,5]. There are various flammable and explosive substances in chemical enterprises, and explosions and fires caused by accidental leaks can result in casualties, environmental damage, and economic losses [6,7]. Therefore, the study of the explosion mechanism of chemical materials is of great significance.

A large number of scholars have studied the explosion mechanism of combustible gas [8-11]. Maria Mitu *et al.*[12] studied the effect of different initial conditions on the explosion characteristics of ethane air mixtures and found that the P_{max} and $(dP/dt)_{max}$ were linearly correlated with the initial pressure when the initial composition and initial temperature were constant. Venera Giurcan *et al.* [13] studied the explosion characteristics of n-butane gas under different initial conditions and found that at a constant initial temperature, the P_{max} and $(dP/dt)_{max}$ were linearly correlated with the initial pressure. Under constant pressure, the $(dP/dt)_{max}$ is independent of temperature changes. Zheng *et al.* [14] studied the explosion characteristics of premixed H_2/Air mixtures using a transparent explosion tube. Cao *et al.* [15], conducted a premixed hydrogen explosion pressure relief test and found that the faster the flame propagation speed, the higher the explosion pressure. Chen *et al.* [16] found that ethylene gas under high oxygen conditions has more obvious maximum pressure rise rate, maximum pressure, and combustion speed. Maria Mitu *et al.* [17] conducted explosion tests on ethane–air mixtures under different initial conditions and found that the flame propagation velocity was similar to the numerical simulation structure. Through the above research, it has been found that the explosion characteristics of combustible gases exhibit different patterns under different conditions. However, only single combustible gases have been studied, and the explosion characteristics of multi-component mixed combustible gases are more complex. Therefore, research on multi-component mixed combustible gases is essential.

Wang *et al.* [18,19] studied the explosive behavior of mixed gases under poor and rich stoichiometric conditions. Shen *et al.* [20] studied the explosion characteristics of methane–ethane mixture and found that its explosion characteristics were obviously similar to those of single-component alkane gas, but the P_{max}, explosion upper limit, and detonation index of methane–ethane mixture increased significantly. Luo *et al.* [21] studied the explosion process of methane/ethane at different yield ratios and obtained three explosion stages of premixed systems. Liu *et al.* [22] conducted a hydrogen/methane/air mixture explosion test in a closed container, and found that the cracks on the flame surface decreased significantly with the increase of methane proportion when the equivalent ratio was the same. Wu *et al.* [23] studied the propagation velocity of explosion flame by observing the spherical flame of n-butane/dimethyl ether mixed gas. Li *et al.* [24] studied the lean H_2/CH_4/air premixed gas, and concluded through the comparison of experiment and numerical calculation that the change of heat loss had an important impact on the explosion pressure and temperature of the whole reaction of premixed gas. Most of the above studies focus on binary combustible gases, and there are many types of volatile gases in petroleum, with approximately four main gases. Therefore, the explosion characteristics of petroleum volatile gases are more complex, and the explosion mechanism is not yet clear, requiring extensive experimental research to analyze and study them.

This article addresses the above issues by studying the explosion pressure and flame propagation of petroleum volatile gases with different equivalence ratios, and discussing the evolution and mechanism of explosions in closed containers. The aim is to reveal the explosion characteristics and mechanisms of petroleum volatile gases,

*Corresponding author:
E-mail address: relax_wxr@163.com (X. Wei)

Received: 10 September, 2024 **Accepted:** 15 December, 2024 **Epub Ahead of Print:** 11 March 2025 **Published:** 18 March 2025
DOI: 10.25259/AJC_12_2024

which has significant theoretical guidance for dealing with petroleum volatile gas explosion accidents.

2. Materials and Methods

2.1. Experimental material

By consulting existing data on the determination of petroleum volatile gas components, a main component and proportion of petroleum volatile gas were selected for experimentation. However, due to the extremely low content of aromatic hydrocarbons and other substances, most of which are liquids, this article does not consider it [25]. The proportion of ethane, propane, n-butane, and isobutane in petroleum volatile gas is set at 4%, 36%, 44%, and 16%, respectively. The matching parameters of each equivalent experimental gas are shown in Table 1. The purity of each gas component is ≥99.9%.

2.2. Test methods for explosion characteristics

This experiment aims to study the characteristic parameters of petroleum volatile gas explosion. A visualized 20 L spherical explosion device was used to conduct petroleum volatile gas explosion experiments under different equivalence ratios. The experimental device system composition is shown in Figure 1. Including a 20 L spherical explosive canister, pulse ignition system, gas distribution system, pressure data acquisition instrument and computer synchronous control system, and vacuum pump [26,27]. The explosion pressure detection range is 0.1～4 MPa, the resolution is 0.001 MPa, the response time is less than 1ms, and the maximum working pressure is 10 MPa. The data acquisition system is configured with 4 channels, and the experimental device automatically evacuates according to the set parameters, automatically adds combustible gas samples into a 20 L explosion container, automatically ignites, and automatically collects explosion parameters and stores them in a data file. The experimental steps are as follows: first, connect the gas cylinder to the air inlet, open the pressure valve of the gas cylinder, set the experimental concentration according to Table 1, and then the system will automatically dispense gas and ignite the electric spark. The arc voltage is 15 KV and the arc current is 20 mA. Each group of experiments will be conducted 5 times.

Table 1. 0.6-1.4 Gas mixture ratio parameter table under the equivalent ratio.

Proportion of components/Equivalent ratio	0.6	0.8	1.0	1.2	1.4
C_2H_6	0.08	0.11	0.14	0.17	0.19
C_3H_8	0.75	1.00	1.25	1.50	1.75
n-C_4H_{10}	0.92	1.22	1.53	1.83	2.14
iso-C_4H_{10}	0.33	0.44	0.56	0.67	0.78
Air	97.92	97.23	96.52	95.83	95.14

2.3. Test method of flame propagation characteristics

The flame propagation experiment of petroleum volatile gas under different equivalent ratio conditions was carried out by using the visualized gas explosion flame propagation experimental device, and the relevant law of flame propagation was obtained. The device system composition is shown in Figure 2, including a visual flame propagation experimental device and a high-speed photography system. Before the experiment began, compressed air and combustible gas were divided into aluminum foil collection bags and connected to air intakes 1–4 of experimental equipment, respectively. According to Table 1, set the experimental parameters and automate the equipment operation. First, clean the exhaust gas in the pipeline, then evacuate and automatically distribute gas, and finally ignite with an electric spark. The arc voltage is 15 KV and the arc current is 20 mA. The high-speed photography system (with a frame rate of 1000 frames per second) synchronously records the propagation process of flames in a glass tube.

3. Results and Discussion

3.1. Study on explosion characteristics of petroleum volatile gases under different equivalent ratios

It can be seen from Figure 3 that the variation trend of the oil volatile gas explosion pressure curve is relatively similar, the blue curve represents “maximum explosion pressure (P_{max})”, and the orange curve represents “maximum rate of pressure rise $(dP/dt)_{max}$”. When the equivalent ratio φ is 0.6, the P_{max} is 0.407 MPa and $(dP/dt)_{max}$ is 16.666 MPa/s. When φ=0.8, the P_{max} of 369.2 ms is 0.798 MPa, and the $(dP/dt)_{max}$ is 18.333 MPa/s. When φ=1.0, the maximum explosion pressure reaches 0.850 MPa at 343.8 ms after ignition, and $(dP/dt)_{max}$ is 29.861 MPa/s. The equivalent ratio of the above reactions is less than or equal to 1.0. At the current stage, the oxygen in the container is abundant, and the petroleum volatile gas can completely react with O_2 to generate CO_2 and release all the energy. Therefore, in the case of oxygen abundance, the intensity of the explosive reaction is determined by the concentration of combustible gas. However, different from the ideal state, when φ=1.2, the P_{max} in this experiment appears, and the P_{max} reaches 0.896 MPa with the shortest time of 321.8 ms, and $(dP/dt)_{max}$ is 28.332 MPa/s. The P_{max} when the equivalence ratio is 1.2 is greater than the P_{max} when the equivalence ratio is 1.0. This is due to the energy generated by a gas explosion inside a sealed container, which is partially converted into pressure and temperature increase, and partially transferred to the container wall through the heat exchange effect. The heat transferred to the container wall during the explosion process is called explosion heat loss. When the reaction equivalence ratio is 1.0, the combustible gas reacts completely with oxygen, but due to the influence of heat loss, its explosion pressure does not reach its maximum value. When the reaction equivalence

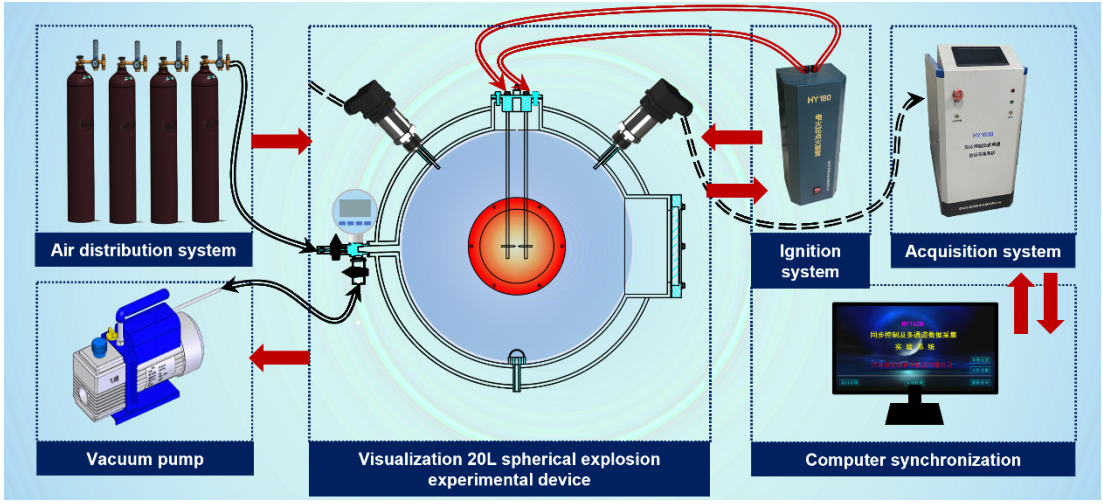

Figure 1. Visualize the 20 L spherical explosive device system composition.

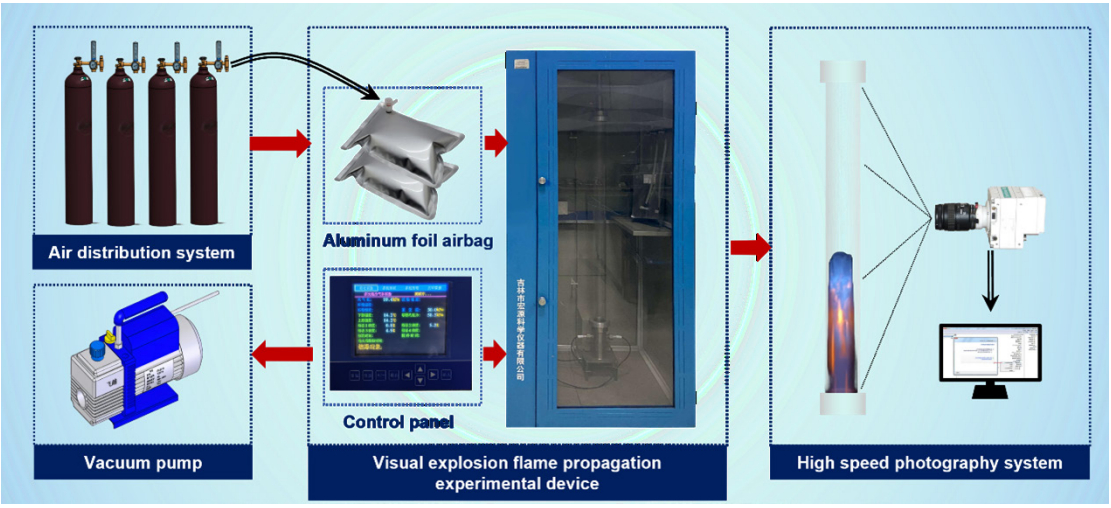

Figure 2. Composition of visualized gas explosion flame propagation device system.

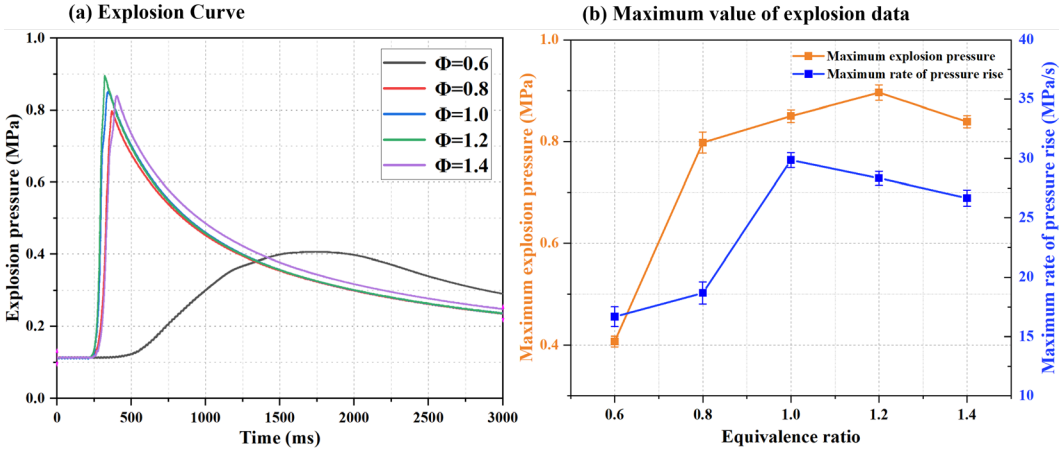

Figure 3. Oil gas explosion pressure curve. (a) Explosion Curve; (b) Maximum value of explosion data. The blue curve represents "maximum explosion pressure (Pmax)", and the orange curve represents "maximum rate of pressure rise (dP/dt)max".

ratio is 1.2, the relatively abundant combustible gas promotes the explosion, causing the maximum explosion pressure of the gas to reach its maximum value. When φ=1.4, the arrival time of the P_{max} lags, and the P_{max} reaches 0.839 Mpa and $(dP/dt)_{max}$ is 26.667 MPa/s at 400.6 ms. At this time, due to the large difference in the ratio between the oxygen content in the container and the volatile gas content of petroleum, the volatile gas of petroleum cannot fully react and release all energy, so the P_{max} falls, and the peak pressure arrival time is also delayed. With the constant increase of the equivalent ratio, the P_{max} presents a trend of first rising and then decreasing, and the arrival time presents a trend of first shortening and then extending.

At this time, due to the low content of petroleum volatile gas in the container, the fuel released insufficient heat in the initial combustion stage, and the subsequent explosion reaction was relatively mild. And its explosion curve rose slowly until it reached the maximum explosion pressure at 0.41 MPa. After this, because the fuel in the reaction vessel did not react completely, the explosion pressure decreased in a very slow trend.

3.2. Study on flame propagation characteristics of petroleum volatile gas with different equivalent ratios

3.2.1. Evolution of flame structure

As shown in Figure 4, the flame propagation trend under all equivalent ratios presents an "N" type. The flame deflagration results in the reduction of combustible gas and oxygen content near the electrode, and the flame shock wave caused by deflagration is reflected from top to bottom, resulting in the flame front regurgitating to the ignition electrode due to the reaction pressure drop and reflected wave. At this time, the flame energy, combustible gas concentration, and oxygen concentration are not enough to support the flame to continue to maintain the detonation state, and the flame presents a relatively short turbulent state.

When φ= 0.6, the brightness of the petroleum volatile gas explosion flame is relatively dark. After the petroleum volatile gas is ignited, the spherical flame is gradually formed in the initial stage, and the explosion flame spreads along the bottom of the pipeline to the top. At this time, the flame is ellipsoidal and the shape is relatively regular. The ellipsoid shape of the flame front gradually becomes sharp, but due to the low concentration of the mixed paraffin fuel, the flame develops slowly in the early stage and the propagation height is low. With the development of the explosion, the curvature of the flame front tends to be gentle, and when the flame continues to propagate upward, it propagates upward in a stable combustion state. At this time, the flame shape becomes ellipsoid, and the flame brightness decreases obviously with the gradual reduction of flammable paraffin content. When the equivalent ratio is 0.8, the flame brightness of the petroleum volatile gas explosion becomes obviously brighter. At the beginning, the flame elongates from an ellipsoid shape to form a typical fingertip flame front. Later, due to the reflection of the flame shock wave to the flame front, a flat-shaped flame is formed. Due to the pressure oscillation in the

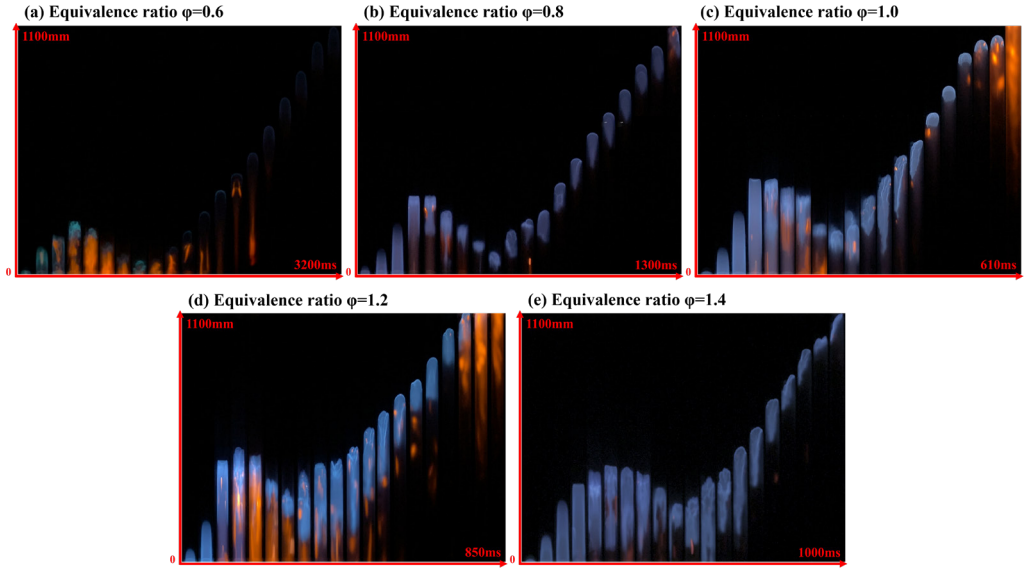

Figure 4. Image of flame propagation. (a) Equivalence ratio φ = 0.6; (b) Equivalence ratio φ = 0.8; (c) Equivalence ratio φ = 1.0; (d) Equivalence ratio φ = 1.2; (e) Equivalence ratio φ = 1.4.

tube, a transient turbulent flame appears, but the typical tulip-shaped flame is not formed in this state. Since then, the pressure propagation gradually becomes stable, and when the flame spreads upward to the top in the shape of water droplets, the laminar flame will be turbulent under the influence of the top pressure due to the closed pipe at the top.

When φ= 1.0, the flame formed is spherical and diffuses outward in a very short time, and is constrained by the tube wall to form a regular symmetrical ellipsoidal flame. There is an obvious highlight area at the lower edge of the flame front, where the upper and lower ends of the shock wave squeeze, resulting in energy accumulation. Due to the abundance of combustible gas, the lowest point reached by the flame is obviously higher than in the first two experiments. The flame continued to spread upward, and then the shape of the flame front began to change from irregular to flat, and then the flame front began to sag downward from the center, but the flame continued to stretch on the pipe wall, forming a typical tulip-shaped flame front. During this period, the flame spread slowly, and the central depression gradually expanded and shifted until the tulip-shaped flame disappeared. The flame continues to rise, and the brightness at the end of the flame is disturbed. The reason for this phenomenon is that in the process of flame propagation, the reaction of petroleum volatile gas at the bottom of the pipeline gradually ends, and turbulence occurs until the flame spreads to the top of the pipeline, and the flame propagation of petroleum volatile gas explosion finally ends.

When φ= 1.2, the flame propagation pattern of petroleum volatile gas is similar to the flame propagation pattern under the optimal equivalent ratio. However, in the process of flame propagation, due to the small volume of the pipeline in the equipment, the uniform gas distribution and the obvious change in oxygen content, the flame brightness is lower than the reaction brightness under the optimal equivalent ratio. The tulip-shaped flame could not be sustained for a long time, and the flame shifted to the right side of the pipeline significantly in the late stage, and the propagation rate of the right side flame front accelerated. The flame propagation tends to be stable, and the flame appears on an ellipsoidal front. At the end of the reaction, oxygen is continuously consumed by the mixed alkanes, and the remaining mixed gas cannot react completely. The flame tail length is significantly less than the flame tail length under the optimal equivalent ratio condition. When φ= 1.4, the oil volatile gas in the explosion flame propagation process, due to the violent reaction in the early stage, resulting in drastic changes in the pressure in the pipeline, and the oxygen in the later stage of propagation is difficult to maintain the flame propagation in the form of laminar flow, and finally propagate to the end of the pipeline in the form of turbulence.

Based on the propagation process of the oil volatile gas explosion flame of the above concentrations, it can be seen that the flame will have a series of changes of different degrees when the oil volatile gas is propagated in the smooth wall pipeline. Generally, its propagation process is divided into four different stages, namely, the “hemispherical” initial stage flame, the “fingertip” early stage flame influenced by the tube wall, the “flat” middle stage flame influenced by the combined action of pressure and wall surface, and the “tulip-shaped” late stage flame finally appeared after the front invaginates. There are four typical flame propagation patterns in each equivalent ratio of petroleum volatile gas explosion, but the flame morphology of the petroleum mixture is still different in the flame inversion stage. As the intact “tulip-flame” continues to propagate forward and collapse, the flame folds more, and the instability triggered by the flame front and pressure wave causes the flame front to form a new “tulip” lip, with a multi-layered structure. The deformed and twisted “tulip-flame” observed when φ is less than 1, and the multilayer structure is not obvious. When the equivalence ratio φ is greater than 1.0, the shape of the explosion flame of petroleum volatile gas shows significant distortion and deformation. At an equivalent ratio 1.0, the tip of the typical tulip flame is more elongated and the “tulip-flame” shape is more full compared to other equivalent ratios.

3.2.2. Flame propagation speed of petroleum volatile gas

Flame propagation speed is also one of the important indexes used to evaluate the flame propagation law. Through the processing and analysis of the flame propagation image, the special position time of the flame and the flame front velocity under different equivalent ratios are obtained. When φ= 1.0, the time for the flame to reach each stage is the shortest, and the time is gradually extended with the increase or decrease of the φ, which is because under this equivalent condition, the oxygen and combustible gas in the pipeline can react exactly completely, and the severity of the reaction is the highest.

Figure 5 shows the average pre-peak flame velocity under different equivalent ratios. The flame mainly goes through three different stages in the propagation process, and the propagation time of each stage is quite different. Where, black curve is the average speed of flame propagation from the ignition time to the highest point in the early forward development stage. The flame propagation speed in this process is significantly higher than that in other stages. This is because in the early stage of flame propagation, the petroleum volatile gas in the pipeline, under the action of high-temperature heat source, violently reacts and burns, and constantly releases heat, promoting the front low-temperature combustible gas to accelerate the reaction and release heat, so that the flame continues to accelerate propagation. When the equivalent ratio is 1.0, the maximum average propagation speed of the flame front reaches 244.6 m/s, which is 1–3 times that of

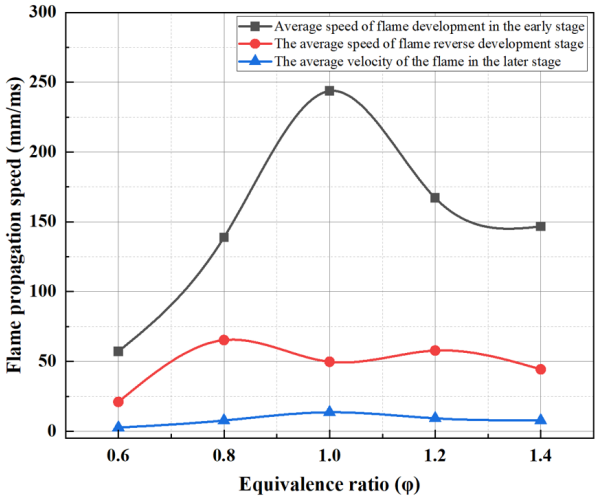

Figure 5. Average velocity curve of flame forward with different equivalent ratio.

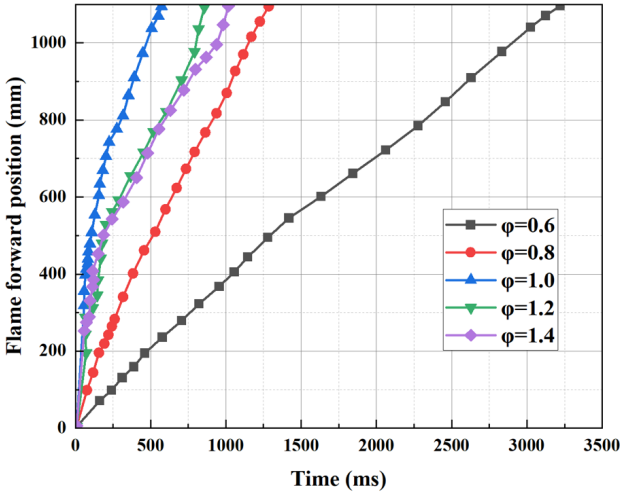

Figure 6. Forward position and time curve of stable transmission phase of different equivalent ratio.

other equivalent ratios. Curve B shows the average speed of flame in the reverse. The red curve in Figure 5 represents the average velocity of the flame in the reverse development stage. The reason for the reverse development is that the superimposed shock wave generated by the violent reaction of the gas in the previous stage propagates to the top of the pipeline, and is reflected by the wall to the flame front propagating upward at the bottom of the pipeline. At this time, due to the large pressure difference before and after the flame front, the flame exhibits reverse propagation. It can be found from the figure that the velocity curve presents an M-shaped distribution, which is due to the difference in equivalent ratio, the intensity of the gas reaction and the total energy released per unit time, and the resulting pressure difference ultimately acts on the flame front. When φ=1.0, the flame front position decreases by 37%. When the equivalent ratio is 0.6 and 1.4, the flame front position decreases by 75% and 50%, respectively. The blue curve shows the average velocity in the late forward flame development stage, during which the reaction gradually becomes stable, the average flame propagation velocity decreases significantly, and the V_{max} appears when the equivalent ratio is 1.0.

Figure 6 shows the trend diagram of the change of the position of the flame front in the later stage of stable flame propagation with time under different equivalent ratios. In this stage, the flame shape will change from “tulip shape” to “hemispherical shape.” When the equivalent ratio is 0.8–1.4, the variation trend of the flame front position over time is roughly the same. Combined with the correlation analysis of flame propagation images under different equivalent ratios, it is found that in the early stage of this stage, the flame propagates upward along one side of the tube wall in an unstable “tulip shape,” and then the pressure at the upper and lower end of the flame front gradually becomes stable until the end. When the equivalent ratio is 0.6 and 1.4, due to the large difference in the content of oxygen and fuel, and the content of fuel and oxygen in the container at this stage has been consumed to a certain extent, the intensity of the reaction is greatly reduced, so that the flame is propagated upward in a stretched “hemispherical” form. When the equivalent ratio is near 1.0, affected by the intensity of the reaction, the flame propagation speed is the fastest, the time is the shortest, and the flame color is the brightest.

In summary, the flame propagation speed of petroleum volatile gas in the propagation process is closely related to the equivalent ratio, and is ultimately determined by the intensity of the reaction. When φ=1.0, the overall flame propagation speed is the fastest, and when the equivalent ratio is gradually less than or greater than 1.0, the flame propagation speed also decreases with the change of the equivalent ratio. However, the reduction degree is not symmetrical distribution with 1.0 equivalent ratio as the center, but when the fuel is relatively rich, because it has little influence on the intensity of combustion reaction in the pipeline, the flame propagation speed near the equivalent ratio of 1.0–1.4 is higher than that near 0.6–1.0.

3.3. Petroleum volatile gas explosion mechanism

Petroleum volatile gas explosion in confined space mainly has three stages, the first stage is the slow reaction stage: the explosive reaction of petroleum volatile gas is in the beginning stage, only part of the alkane gas participates in the reaction, the heat generated is less, and the pressure curve does not increase significantly. The second stage is the rapid surge stage, in which the detonation of combustible gas occurs. Due to the continuous reaction and heat release of the reactants in the early stage, the heat in the container accumulates, and a large number of combustible gases participate in the reaction, resulting in P rising sharply and reaching the peak in a short time. The third stage is the linear decay stage, the reaction of petroleum volatile gas in the reaction vessel is nearly complete, and a lot of H_2O and CO_2 are generated. The shock wave generated in the early stage is also continuously consumed under the interaction, and the temperature in the container gradually decreases with the heat conduction effect of the wall, and the explosion pressure gradually decays.

In an ideal state, when the equivalence ratio of combustible gas to air is 1.0, it can completely react, release the most heat, and generate the maximum explosive pressure. However, under actual conditions, the gas explosion reaction will be interfered with by many factors. Figure 7 shows the schematic diagram of various heat losses in the gas explosion experiment. First of all, in the process of a gas explosion, heat always follows the basic principle of transfer from the high-temperature region to the low-temperature region, and the greater the temperature difference generated, the more obvious the role of heat transfer and the

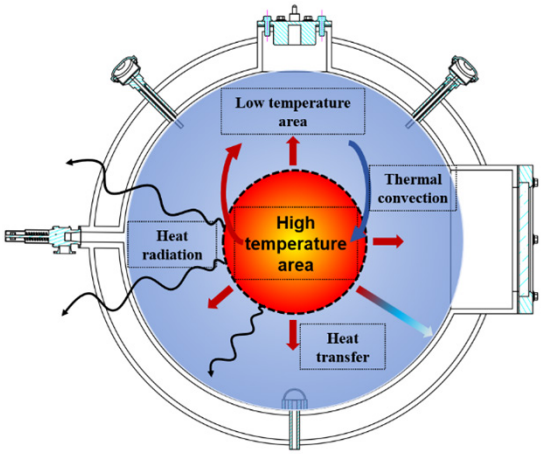

Figure 7. Schematic diagram of explosive heat transfer of oil precipitation gas.

faster the speed. Secondly, because the movement law of the gas used in the experiment in the container belongs to the fluid movement under macro conditions, when the fluid mixing phenomenon occurs at different temperatures, the heat of the high-temperature gas and the heat of the low-temperature gas will be transferred to each other. Especially when the explosive reaction of petroleum volatile gas under the action of high temperature rapid thermal expansion, the spacing of the internal gas molecules will also expand; at this time, the density of the unheated area is higher than the density of the heated area. Therefore, the two parts of the gas will appear in the macroscopic sense of flow. In this study, due to the low temperature of the container wall, it is easy to form heat convection in the tank, resulting in the wall effect of high-temperature gas with the metal inner wall of the container, resulting in heat loss. Finally, another form of heat transmission is the phenomenon of thermal radiation, and the transmission of radiation does not need to be in any medium as a carrier, that is, the form of electromagnetic waves can be emitted to transfer energy to the outside world, and there is heat loss in the process, such heat rays will be absorbed by other substances to increase heat energy, and reflect and transmit part of the rays. The high-temperature gas produced by the explosion loses heat in the three forms mentioned above, and as the temperature continues to rise, the more heat is lost. This eventually results in the loss of heat generated by the chemical reaction at an equivalent ratio of 1.0, which cannot be fully used to accelerate the subsequent reaction, resulting in a decrease in the explosion temperature and its maximum explosion pressure.

4. Conclusions

In this paper, the explosion characteristics and mechanism of petroleum volatile gas are studied by using a 20L spherical explosion experiment device and a visual gas explosion flame propagation experiment device. By comparing the explosion results of six kinds of different equivalent ratios, the difference in explosion characteristics of petroleum volatile gas is obtained. Based on the analysis of explosion characteristics in confined space, the explosion mechanism of petroleum volatile gas is studied. The conclusion can be summarized as follows:

(1) The variation of explosive overpressure of petroleum volatile gas under different equivalent ratios was studied by using a visual 20 L spherical explosive device. Under the condition of different equivalent ratios of petroleum volatile gas, the P_{max} increases first and then decreases, and the arrival time decreases first and then extends. When φ=1.2, the P is the highest and the time to reach the P_{max} is the shortest.
(2) The flame propagation process of petroleum volatile gas was studied by using the visual gas explosion flame propagation experimental device. The results show that the flame propagation at all equivalent ratios is “N” type, because the deflagration shock wave bounces from the top to the bottom and affects the flame front. At the same time, the flame propagation velocity of petroleum volatile gas is closely related to the equivalent ratio. When φ=1.0, the flame propagation speed is the fastest, the flame color is the brightest, and the “tulip-flame” structure is fuller.
(3) The explosion of petroleum volatile gas in confined space mainly includes a slow reaction period, a rapid steep increase period, and a linear decay period, in which the rapid steep increase period produces the main stage of overpressure and heat. In actual working conditions, when φ of combustible gas is 1.0, the explosion pressure is the largest and the heat is released the most. Because part of the heat in the explosive high-temperature gas is lost through heat convection, heat transfer and heat radiation, the subsequent reaction is affected, resulting in the reduction of the explosion temperature and the P_{max}.

CRediT authorship contribution statement

Yansong Zhang: Investigation, Methodology, Software, Writing—original draft, Writing—review and editing. **Yunkuan Zhang:** Conceptualization, Funding acquisition, Writing—review and editing. **Xiang Wang:** Investigation, Project administration, Validation, Visualization. **Jie Zhang:** Conceptualization, Investigation. **Jing Shi:** Formal analysis, Writing—review and editing. **Xiangrui Wei:** Formal analysis, Methodology, Writing—review and editing.

Declaration of competing interest

The authors declare that they have no known competing financial interests or personal relationships that could have appeared to influence the work reported in this paper.

Declaration of Generative AI and AI-assisted technologies in the writing process

The authors confirm that there was no use of AI-assisted technology for assisting in the writing of the manuscript and no images were manipulated using AI.

Acknowledgment

This work was supported by the National Natural Science Foundation of China (Grant No. 52404242) and China Postdoctoral Science Foundation (Grant No. 2024MD753981).

References

1. Chen, C., Wei, J., Zhang, T., Zhang, H., Liu, Y., 2025. Effect of abrasive volume fraction on energy utilization in suspension abrasive water jets based on VOF-DEM method. *Powder Technology* **449**, 120427. doi: https://doi.org/10.1016/j.powtec.2024.120427
2. Ji, S., Lai, X., Cui, F., Liu, Y., Pan, R., Karlovšek, J., 2024. The failure of edge-cracked hard roof in underground mining: An analytical study. *International Journal of Rock Mechanics and Mining Sciences* **183**, 105934. doi: https://doi.org/10.1016/j.ijrmms.2024.105934
3. Yu, X., Meng, X., Chen, J., Zhu, Y., Li, Y., Qin, Z., Ding, J., Song, S., 2024b. Macroscopic behavior and kinetic mechanism of ammonium dihydrogen phosphate for suppressing polyethylene dust deflagration. *Chemical Engineering Journal* **498**, 155320. doi: https://doi.org/10.1016/j.cej.2024.155320
4. Zhang, C., Jin, P., Chen, C., Zhang, X., Zhou, Z., Geng, S., Zhang, Y., Lan, Y., Shi, X., Cao, W., 2023. Flame propagation characteristics and surface functional groups changes of corn starch dust during the combustion process. *Powder Technology* **430**, 118995. doi: https://doi.org/10.1016/j.powtec.2023.118995
5. Zhang, Y., Li, W., Pei, Q., Zhang, X., Zhou, Z., Xu, S., Lan, Y., Jiao, F., Shi, X., Xu, S., Cao, W., 2024. Effect of stearic acid coating on the flame propagation and reaction mechanism of AlH3. *Fuel* **358**, 130140. doi: https://doi.org/10.1016/j.fuel.2023.130140
6. Li, Y., Meng, X., Song, S., Chen, J., Ding, J., Yu, X., Zhu, Y., Qin, Z., 2024. Piperazine pyrophosphate-functionalized Ni-MOF metal framework: Fabrication and synergistic explosion suppression mechanisms. *Chemical Engineering Journal* **499**, 155870. doi: https://doi.org/10.13039/501100001809
7. Yu, X., Chen, J., Meng, X., Zhu, Y., Li, Y., Qin, Z., Wu, Y., Yan, K., Song, S., 2024a. Polyethylene deflagration characterization and kinetic mechanism analysis. *Energy* **303**, 131990. doi: https://doi.org/10.1016/j.energy.2024.131990
8. Wang, K., Su, M., Wei, L., Chen, S., Kong, X., Fang, Y., 2022a. Effect of initial turbulence on explosion behavior of stoichiometric methane-ethylene-air mixtures in confined space. *Process Safety and Environmental Protection* **161**, 583-593. doi: https://doi.org/10.13039/501100001809
9. Oppong, F., Xu, C., Zhongyang, L., Li, X., Zhou, W., Wang, C., 2019. Evaluation of explosion characteristics of 2-methylfuran/air mixture. *Journal of Loss Prevention in the Process Industries* **62**, 103954. doi: https://doi.org/10.13039/501100012166
10. Xu, C., Wu, S., Li, Y., Chu, S., Wang, C., 2020. Explosion characteristics of hydrous bio-ethanol in oxygen-enriched air. *Fuel* **271**, 117604. doi: https://doi.org/10.13039/501100011283
11. Su, Y., Luo, Z., Wang, T., Chen, X., Lu, K., 2022. Effect of nitrogen on deflagration characteristics of hydrogen/methane mixture. *International Journal of Hydrogen Energy* **47**, 9156-9168. doi: https://doi.org/10.1016/j.ijhydene.2022.01.013
12. Mitu, M., Giurcan, V., Razus, D., Oancea, D., 2012. Temperature and pressure influence on ethane—air deflagration parameters in a spherical closed vessel. *Energy Fuels* **26**, 4840-4848. doi: https://doi.org/10.1021/ef300849r
13. Giurcan, V., Mitu, M., Razus, D., Oancea, D., 2017. Pressure and temperature influence on propagation indices of n-butane—air gaseous mixtures. *Process Safety and Environmental Protection* **111**, 94-101. doi: https://doi.org/10.1016/j.psep.2017.06.020
14. Zheng, L., Zhu, X., Wang, Y., Li, G., Yu, S., Pei, B., Wang, Y., Wang, W., 2018. Combined effect of ignition position and equivalence ratio on the characteristics of premixed hydrogen/air deflagrations. *International Journal of Hydrogen Energy* **43**, 16430-16441. doi: https://doi.org/10.13039/501100001809
15. Cao, W., Li, W., Yu, S., Zhang, Y., Shu, C-Min., Liu, Y., Luo, J., Bu, L., Tan, Y., 2021. Explosion venting hazards of temperature effects and pressure characteristics for

premixed hydrogen-air mixtures in a spherical container. *Fuel* **290**, 120034. doi: https://doi.org/10.13039/501100004480
16. Chen, C-Feng., Shu, C-Min., Wu, H-Chun., Ho, H-Hsiu., Ho, S-Ping., 2017. Ethylene gas explosion analysis under oxygen-enriched atmospheres in a 20-liter spherical vessel. *Journal of Loss Prevention in the Process Industries* **49**, 519-524. doi: https://doi.org/10.1016/j.jlp.2017.05.022
17. Mitu, M., Razus, D., Giurcan, V., Oancea, D., 2015. Normal burning velocity and propagation speed of ethane—air: Pressure and temperature dependence. *Fuel* **147**, 27-34. doi: https://doi.org/10.1016/j.fuel.2015.01.026
18. Wang, T., Luo, Z., Wen, H., Cheng, F., Deng, J., Zhao, J., Guo, Z., Lin, J., Kang, K., Wang, W., 2017. Effects of flammable gases on the explosion characteristics of CH 4 in air. *Journal of Loss Prevention in the Process Industries* **49**, 183-190. doi: https://doi.org/10.13039/501100001809
19. Wang, T., Luo, Z., Wen, H., Zhang, J., Mao, W., Cheng, F., Zhao, J., Su, B., Li, R., Deng, J., 2019. Experimental study on the explosion and flame emission behaviors of methane-ethylene-air mixtures. *Journal of Loss Prevention in the Process Industries* **60**, 183-194. doi: https://doi.org/10.13039/501100001809
20. Shen, X., Zhang, B., Zhang, X., Xiu, G., 2017. Explosion characteristics of methane-ethane mixtures in air. *Journal of Loss Prevention in the Process Industries* **45**, 102-107. doi: https://doi.org/10.13039/501100001809
21. Luo, Z., Hao, Q., Wang, T., Li, R., Cheng, F., Deng, J., 2020. Experimental study on the deflagration characteristics of methane-ethane mixtures in a closed duct. *Fuel* **259**, 116295. doi: https://doi.org/10.13039/501100012166
22. Liu, L., Luo, Z., Su, B., Song, F., Wu, P., Wang, T., Deng, J., 2024. Study on the explosion characteristics and flame propagation of hydrogen-methane-air mixtures in a closed vessel. *Journal of Loss Prevention in the Process Industries* **87**, 105224. doi: https://doi.org/10.13039/501100001809
23. Wu, H., Hu, E., Yu, H., Li, Q., Zhang, Z., Chen, Y., Huang, Z., 2014. Experimental and numerical study on the laminar flame speed of n-butane/dimethyl ether—air mixtures. *Energy Fuels* **28**, 3412-3419. doi: https://doi.org/10.13039/501100001809
24. Li, R., Luo, Z., Wang, T., Cheng, F., Lin, H., Zhu, X., 2020. Effect of initial temperature and H2 addition on explosion characteristics of H2-poor/CH4/air mixtures. **Energy** *213*, 118979. doi: https://doi.org/10.13039/501100002858
25. Kang, Y., 2016. Research on determination and migration of volatile gases from the crude oil. China University of Petroleum Master Degree Thesis. https://kns.cnki.net/kcms2/article/abstract?v=MdENDFpkZq7SxAGlbWsYckwR4pCACL_58totMmcHIeKfec1A4ctVS6VVHpmrpCDirb2jRwz20F5cptbbGn3ehcQ6FZJgSBA-OB0SIxLIRDwPZ4r9LQoySP3K-A4ybkkz2VOK8XomlL-W8GyPqUSUY-3l8dSVVyTswPmBof41AyefR1LmO_5wKh7xtGhmau1R-gjgn1BsPdI=&uniplatform=NZKPT&language=CHS
26. Luo, Z-min., Nan, F., Cheng, F.-M., Xiao, Y., Wang, T., Li, R.-K., Su, B., 2024. Study on the inhibition of hydrogen explosion pressure and flame propagation by trifluoroiodomethane. *International Journal of Hydrogen Energy* **49**, 670-680. doi: https://doi.org/10.13039/501100001809
27. Wang, T., Liang, H., Lin, J., Luo, Z., Wen, H., Cheng, F., Zhao, J., Su, B., Li, R., Ding, X., Deng, J., 2022b. The explosion thermal behavior of H2/CH4/air mixtures in a closed 20 L vessel. *International Journal of Hydrogen Energy* **47**, 1390-1400. doi: https://doi.org/10.13039/501100001809